Journal of Cleaner Production 154 (2017) 233–241

Contents lists available at ScienceDirect

Journal of Cleaner Production

journal homepage: www.elsevier.com/locate/jclepro

Sustainable production of high purity curcuminoids from *Curcuma longa* by magnetic nanoparticles: A case study in Brazil

Maria Izabela Ferreira [a, 1], Massimiliano Magro [b, c, 1], Lin Chau Ming [d], Monica Bartira da Silva [d], Luan Fernando Ormond Sobreira Rodrigues [d], Débora Zanoni do Prado [a], Emanuela Bonaiuto [b], Davide Baratella [b], Jessica De Almeida Roger [b], Giuseppina Pace Pereira Lima [a], Monica Rossetto [e], Lucio Zennaro [e], Fabio Vianello [b, c, *]

[a] Department of Chemistry and Biochemistry, São Paulo State University (UNESP), Institute of Biosciences, Botucatu, São Paulo, CP 510, 18.618-970, Brazil
[b] Department of Comparative Biomedicine and Food Science, University of Padua, Padua, Italy
[c] Regional Centre of Advanced Technologies and Materials, Department of Physical Chemistry and Experimental Physics, Faculty of Science, Palacky University, 17 Listopadu 1192/12, 771 46 Olomouc, Czech Republic
[d] Department of Horticulture São Paulo State University (UNESP), School of Agriculture, Botucatu, São Paulo, CP 510, 18.618-970, Brazil
[e] Department of Molecular Medicine, University of Padua, Padua, Italy

ARTICLE INFO

Article history:
Received 24 January 2017
Received in revised form
23 March 2017
Accepted 29 March 2017
Available online 31 March 2017

Keywords:
Turmeric
Curcumin production
Curcumin purification
Magnetic purification
Magnetic nanoparticles
Biomass reduction

ABSTRACT

Large volumes of residual biomass could represent a matter of concern for large-scale purification of natural compounds, heavily influencing processing industries and logistic sizing, amount of solvents employed for the extraction processes and the final chemical and biological waste generation. In the present study, carried out in Brazil, the production of curcuminoids in *Curcuma longa* L. rhizomes was maximized as a function of plant maturity and solar UV exclusion. Noteworthy, curcuminoid content reached its maximum at around the end of the early vegetative phase (65 days after planting), henceforward plant growth determined only a detrimental accumulation of wastes. The harvesting at this early phase of plant maturation led to a more than tenfold reduction of exceeding biomass. In addition, by means of an innovative, sustainable and high efficient magnetic purification process for curcuminoids based on Surface Active Maghemite Nanoparticles (SAMNs), an outstanding yield of 90% and >98% purity, were achieved in a single magnetic purification step. The formation of the SAMN-curcuminoid complex (SAMN@curcuminoid) was demonstrated by optical and electron spin resonance spectroscopy and electron microscopy. The scalability of the purification method was proved by the application of an automatic modular pilot system for continuous magnetic purification of curcuminoids, capable of managing 100 L day^{-1} of SAMN@curcuminoid suspensions. The presented multidisciplinary approach embodies the fundamental principles of cleaner production providing a paradigm for the utilization of magnetic nanoparticles for biomolecule purification. Moreover, Brazilian agro-industries can benefit from sustainable innovation strategy outlined by the current study.

1. Introduction

The rational use of natural resources, the minimization of wastes as well as the sustainable product innovation are prerogatives of the research field on cleaner production. *Curcuma longa* (Zingiberaceae), also known as turmeric, is the most important source of curcuminoids, comprising curcumin and two related compounds, demethoxycurcumin (DMC) and bisdemethoxycurcumin (BDMC) (Kulkarni et al., 2012). Nowadays, curcumin is used as a food supplement in several countries and the molecular basis for its pharmaceutical application has been already delineated for a wide range of diseases (Gupta et al., 2013). For this reason, curcumin and

* Corresponding author. Department of Comparative Biomedicine and Food Science, University of Padua, Agripolis - Viale dell'Università 16, Legnaro, 35020, PD, Italy.
E-mail address: fabio.vianello@unipd.it (F. Vianello).
[1] Authors contributed equally to this work.

http://dx.doi.org/10.1016/j.jclepro.2017.03.218
0959-6526/

its derivatives are attracting an increasing interest in food and pharmaceutical field. Thus, the development of strategies for the improvement of pure curcuminoid production, from plant cultivation to molecule isolation, represents an important task. From this viewpoint, the influence of environmental factors and agronomic techniques on plant cropping is an important research topic, as these factors influence the accumulation of biomass as well as the biosynthesis of bioactive compounds.

In the present report, in the specific agro-climatic zone, under the effect of different light intensities and UV exclusion, the curcuminoid content in rhizomes reached its maximum at approximately the end of the early vegetative phase. Henceforward, the amount of curcuminoids did not significantly vary with plant growth. Thus, the anticipation of the harvest led to a significant waste minimization and a one order of magnitude lower biomass accumulation. Moreover, a sustainable and competitive purification procedure was developed in the present study. Pharmaceutical and food industries usually employ various chromatographic, ultrafiltration, or precipitation techniques or solvent extraction methods for isolating biomolecules of interest (Kitts and Weiler, 2003). These techniques show significant drawbacks when applied at the industrial scale, such as expensive instrumentation, time-consuming procedures, or large quantities of organic solvents and corresponding wastes. In particular, the main disadvantage of all standard column liquid chromatography procedures is the impossibility to cope with biological samples containing particulate material, so these techniques are not suitable for working at the early stages of the isolation/purification process, when suspended solids and fouling components are present in the sample (Turková, 1978). In this context, the use of magnetic nanoparticles can represent a valuable option as well as an innovation opportunity for cleaner production. Notwithstanding, most of the proposed syntheses of magnetic nanoparticle drastically limit their exploitation at an industrial level, as they are characterized by difficult scalability, impressive consumption of organic solvents, high costs and heavy impact on the environment. Furthermore, magnetic nanoparticles need in the most of the cases, to be stabilized to avoid self-aggregation and to guarantee long-term stability, pH and electrolyte tolerance, and proper surface chemistry. Coating processes are often cumbersome, time-consuming, and expensive, with low yields and, due to their lack of stability, coating tend to degrade. Coating deterioration represents a drawback as this phenomenon compromises the binding capability of the material. As a consequence, the use of nanomaterials as means for cleaner production could reasonably become a paradox, as they represent themselves sources of environmental hazard.

Recently, we developed a novel synthetic procedure for magnetic nanomaterial in the size range around 10 nm, constituted of stoichiometric maghemite (γ-Fe_2O_3) and showing peculiar surface chemical behavior, called surface active maghemite nanoparticles (SAMNs) (Magro et al., 2015a). Noteworthy, SAMNs applicability range from the biomedical field, as a long-term imaging nanoprobes (Cmiel et al., 2016; Skopalik et al., 2014), to the advanced material development, such as conductive DNA based metamaterials (Magro et al., 2015b) and electrocatalysis (Magro et al., 2016a), as well as in sensoristics (Urbanova et al., 2014) for the determination of glucose (Baratella et al., 2013), polyamines (Bonaiuto et al., 2016) and hydrogen peroxide (Magro et al., 2013, 2014a). SAMNs present a high average magnetic moment and high water stability as colloidal suspensions without any superficial modification or coating derivatization. Because of their unique physical and chemical properties, these naked iron oxide nanoparticles are currently used to immobilize various biomolecules, such as avidin (Magro et al., 2012a), curcumin (Magro et al., 2015c), citrinin (Magro et al., 2016b), rhodamine B isothiocyanate (Sinigaglia et al., 2012) and endogenous proteins from prokaryotes and eukaryotes (Magro et al., 2016c; Miotto et al., 2016; Venerando et al., 2013). Thus, SAMNs represent an ideal material for cleaner production as their synthesis is scalable and completely carried out in water. They do not need any kind of stabilizing coating, present a very high aqueous colloidal stability and, in contrast to their surface reactivity, they are structurally conserved upon binding to target molecules, such as curcumin (Magro et al., 2014b), DNA (Magro et al., 2015b) and chromate (Magro et al., 2016e).

In the present work, a purification method leading to the recovery of curcuminoids present in the mother biological matrix with high yield (90%) and purity (98%) was proposed. In addition, the feasibility of the proposed approach to be scaled up at industrial level was demonstrated by developing an automatic modular pilot plant, which was able of performing the continuous curcuminoid purification from the initial water-ethanol extract. The reported multidisciplinary approach, ranging from agronomy to nanotechnology and engineering, offers valuable insights for a sustainable production of pure curcuminoids at an industrial scale and for the economic valorization of Brazilian agro-industry.

2. Materials and methods

2.1. Materials

The cultivation experiments were carried out in an experimental farm of the Agronomic Science College, Universidade Estadual Paulista - UNESP, Botucatu - SP, in São Manuel - SP (22°46′0,571″ S and 48°34′11,32″ W, 744 m above sea level).

The experimental design was completely randomized with five light conditions and four harvest times, split plot in time, with five replicates consisting of six plants. Light levels were: A) UV exclusion; B) full sun, C) 30% shading; D) 50% shading and E) 70% shading. Harvest times were: 65, 128, 174, and 203 days after planting (DAP) corresponding to January, April, May, and June 2013.

The different light conditions were obtained by protected environments in tunnel structures, 3 m wide, 1.70 m high and 22.5 m long, with different coatings for light exposure control. The coating applied to exclude UV radiations was an anti-UV polyethylene film (150 μm) (Trifilme, Plastilux, Brazil), characterized by excluding more than 80% UV-B radiation. Coatings used to control shading levels were black polyethylene screens with 30%, 50% and 70% shading (Plastilux, Brazil).

An infrared gas analyser (LI-6400, Li-Cor Inc. Lincholn, NE, USA) was used to quantify photosynthetically active radiation (PAR). Measurements were carried out at 09:00 and 11:00 a.m. in cloudless days, every month during the plant growth. The mean PAR measured was used to define the amount of radiation for each light exposure condition: UV exclusion (610 μmol $m^{-2}s^{-1}$), 70% shading (360 μmol $m^{-2}s^{-1}$), 50% shading (500 μmol $m^{-2}s^{-1}$), 30% shading (630 μmol $m^{-2}s^{-1}$) and full sun (1200 μmol $m^{-2}s^{-1}$).

The soil was classified as Oxisol, sandy phase (Camargo et al., 1987; Santos et al., 2006) and exhibited the following chemical characteristics in the layer between 0 and 0.20 m: 12 g dm^{-3} organic matter; pH 5.4; 204 mg dm^{-3} P; 2.5 mmol dm^{-3} K; 39 mmol dm^{-3} Ca; 11 mmol dm^{-3} Mg; 71 mmol dm^{-3} CTC; $V = 76\%$.

Seed rhizomes, 12 cm long, were selected and homogenized. Planting was carried out on plots 0.4 m high, spaced 0.5 m apart, by placing each propagule 4 cm deep.

Necessary crop treatments, such as weed control and repairs in ridges were carried out during plant growth. Plots were irrigated daily, according to water demand recorded by tensiometers, thus soil was near its calculated field capacity. Irrigation was suspended 15 days before harvest.

Rhizomes of six plants for each replica were harvested, sliced and dried in a forced air-circulating oven at 65 ± 5 °C until the samples reached a constant weight to determine biomass production, expressed per plant. These dried rhizomes were milled to a fine powder, pooled, mixed and used to measure the curcuminoid content by HPLC. The water content in the fresh rhizomes was approximately 83 ± 3%.

2.2. Chemicals

Chemicals were purchased at the highest commercially available purity, and were used without further treatment. Iron(III) chloride hexahydrate (97%), sodium borohydride ($NaBH_4$), and ethanol (99.6%) were obtained from Aldrich (Sigma-Aldrich, Italy) as well as pure curcuminoids (curcumin, demethoxycurcumin, and bis-demethoxycurcumin) (purity ≥ 94.0%), being curcumin ≥80.0% (by TLC). HPLC grade ethanol, acetonitrile and acetic acid were from Mallinckrodt (St. Louis, USA).

2.3. Instrumentation

Optical spectroscopy measurements were performed in 1 cm quartz cuvettes using a Cary 60 spectrophotometer (Varian Inc., Palo Alto, CA, USA).

Electron spin resonance spectra were acquired in water, in a glass tube (50 μL), at room temperature (21 °C), by a Bruker ER200D X-band ESR spectrometer (Bruker, Germany). Experimental parameters were: magnetic field modulation 100 kHz; power, −10 dB (20 mW); frequency, 9.84 GHz; scan rate, 20 Gauss s^{-1}; modulation amplitude, 1 Gauss; time constant, 1 s. The center field values were calibrated and locked by using the stable free radical 2,2-diphenyl-1-picrylhydrazyl (DPPH), 50 μM, as internal standard.

A series of Nd − Fe − B magnets (N35, 263–287 kJ/m^3 BH, 1170–1210 mT flux density by Powermagnet, Germany) was used for the magnetic driving of nanoparticles.

2.4. Synthesis of surface active magnetic nanoparticles

A typical synthesis of nanoparticles was already described and can be summarized as follows (Magro et al., 2012b, 2015a): $FeCl_3 \cdot 6H_2O$ (10.0 g, 37 mmol) was dissolved in Milli-Q grade water (800 mL) under vigorous stirring at room temperature. $NaBH_4$ solution (2 g, 53 mmol) in ammonia (3.5%, 100 mL, 4.86 mol mol^{-1} Fe) was quickly added to the mixture. Soon after the reduction reaction occurrence, the temperature of the system was increased to 100 °C and kept constant for 2 h. Then, the material was cooled at room temperature and aged in water, as prepared, for 24 h. This product was separated by imposition of an external magnet and washed several times with water. This material can be transformed into a red-brown powder (final synthesis product) by drying and curing at 400 °C for 2 h. The resulting nanopowder showed a magnetic response upon exposure to a magnetic field. The final mass of product was 2.0 g (12.5 mmol) of Fe_2O_3, and a yield of 68% was calculated.

The nanoparticulated resulting material was characterized by Mössbauer spectroscopy, FT-IR spectroscopy, high-resolution transmission electron microscopy, x-ray powder diffraction, and magnetization measurements and was constituted of stoichiometric maghemite (γ-Fe_2O_3) with a mean diameter (d_{av}) of 11 ± 2 nm (Magro et al., 2012b), which can lead to the formation, upon ultrasound application in water (Falc, model LSB1, 50 kHz, 500 W), of a stable colloidal suspension, without any organic or inorganic coating or derivatization. The surface of these bare maghemite nanoparticles shows peculiar binding properties and can be reversibly derivatized with selected organic molecules. We called these bare nanoparticles surface active maghemite nanoparticles (SAMNs). SAMNs are currently produced and delivered by AINT s.r.l. (Venice, Italy).

2.5. Quantitative determination of curcuminoids by HPLC

The determination of bis-demethoxy-curcumin (BDMC), demethoxy-curcumin (DMC) and curcumin was carried out according to He with modifications (He et al., 1998). A UHPLC system (Ultimate 3000 BioRS, Dionex-Thermo Fisher Scientific Inc., USA) equipped with a diode array detector, was used. An Ace 5 C18 (Advanced Chromatography Technologies, UK) column (5 μm, 25 cm × 4.6 mm) was used for curcuminoids analysis, at 48 °C. The gradient profile of the mobile phase, (A) 0.25% acetic acid in water and (B) acetonitrile (HPLC grade), was as follows: 0–17 min, 40–60% B; 17–32 min, 60–85% B; 32–38 min, 85% B; 38–40 min, 85–40% B; 40–45 min, 40% B; the flow rate was 0.5 mL min^{-1}. The injection volume was 20 μL (full loop). All samples were filtered through 0.22 μm membrane filters before the injection. Curcuminoids were identified by retention times as determined with injections tests with standards (curcumin, demethoxy-curcumin, and bisdemethoxy-curcumin).

2.6. Statistical analysis

The experimental results were expressed as mean values (mean ± SE). Data were analyzed using Sigma Plot (version 10.0) and Assistat statistical program (version 7.7). Significant differences between the samples were evaluated by analysis of variance (ANOVA) followed by Tukey test ($p < 0.05$).

3. Results and discussion

3.1. Effect of plant maturity and light conditions on curcuminoid content in C. longa rhizomes

According to literature, the highest curcuminoid content in *C. longa* rhizome can range from 2.7% to 7.7% with respect to the total dry mass (Nair, 2013). Notwithstanding, the correlation between plant maturity and curcuminoid content is still a matter of debate. Authors found that the highest curcuminoid production was reached in plants between 5 and 9 month growth, while others affirmed that plant maturity does not influence curcumin production (Asghari et al., 2009; Cooray et al., 1988; Manhas and Gill, 2012). Furthermore, other studies, already reporting on the influence of light intensity on productivity and quality of turmeric, indicated a good curcumin productivity in *C. longa* under shading (Bhuiyan et al., 2012; Hossain et al., 2009; Padmapriya et al., 2007; Srikrishnah and Sutharsan, 2015). As the aim of the present study was the optimization of curcuminoid production by *C. longa* rhizomes, as well as of their purification yield, focused to a future application at industrial level, besides curcuminoid content, the limitation of plant biomass represents a crucial aspect for cost reduction of raw material transport, waste generation and solvent volumes in the extraction process. Thus, total curcuminoid content in *C. longa* rhizomes was studied as a function of plant maturity and light conditions specifically in a case study (Sao Paulo state, see Materials and Methods) in the Brazilian agroclimatic zone. Curcuminoid concentration in rhizomes, determined by HPLC in extracts, as a function of days after planting (DAP) and light conditions is reported in Fig. 1. Noteworthy, curcuminoid content, expressed in mg per gram rhizome mass, decreased with time for all tested light conditions. In particular, curcuminoid concentration decreased following an exponential decay, and the corresponding first order kinetic constants were calculated for all the light exposure

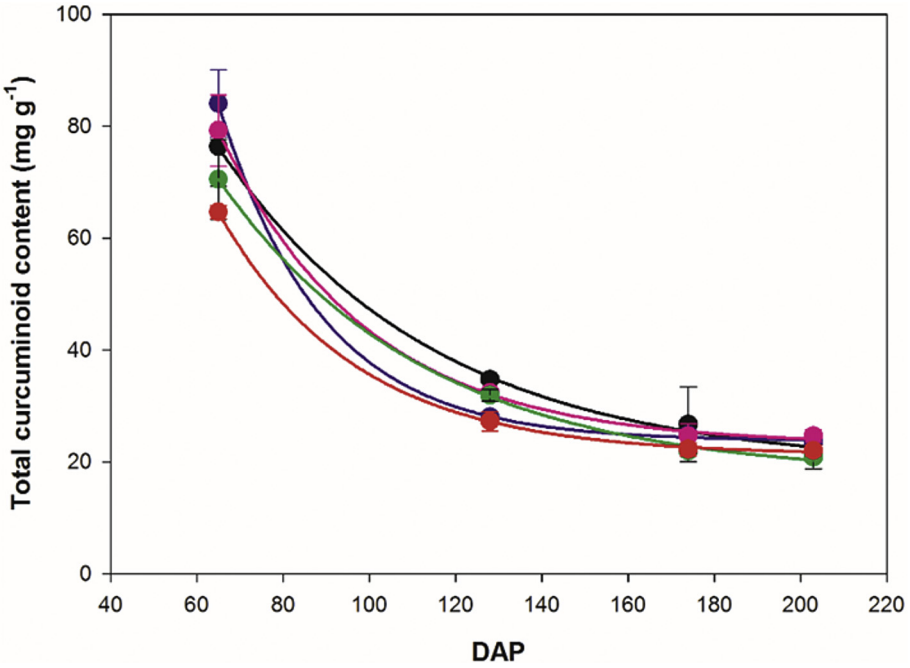

Fig. 1. Curcuminoid content (mg g^{-1}) in rhizome mass as a function of *C. longa* maturity (DAP) under different light conditions. Curcuminoid determinations were carried out by HPLC as described in Materials and Methods. Black line = UV exclusion; blue line = 70% shading; pink line = 50% shading; green line = 30% shading; orange line = full sun. Determinations were carried out in triplicate. The maximum error was below 7.0% for all the experimental points. (For interpretation of the references to colour in this figure legend, the reader is referred to the web version of this article.)

conditions. As model, we assumed a single exponential as shown in the following equation:

$$TCC_{(DAP)} = TCC_{maturity} + TCC_0 \times \exp^{(-k \times DAP)}$$

where $TCC_{(DAP)}$ represents the total curcuminoid content (mg g^{-1}) of *Curcuma longa* in a specific day after planting (DAP), $TCC_{maturity}$ is the total curcuminoid content (mg g^{-1}) at the end of the plant growth. TCC_0 is the extrapolated total curcuminoid content at 0 DAP, k is the decay kinetic constant. Interestingly, no significant differences emerged among decay kinetic constants, which were not sensitive on light exposure: the average value resulted $k = 3.0 \pm 0.2 \times 10^{-2}$ $days^{-1}$. The curcuminoid content reached a plateau after 180 DAP, where it was about 30% with respect to the first determination (65 DAP) (see Fig. 1). Interestingly, at 65 DAP, the influence of light exposure on curcuminoid level was evident. At 65 DAP, curcuminoid content was according to the following order (see Fig. 2): plants under full sun < 30% shading < 50% shading < 70% shading. The exclusion of solar UV radiations resulted in a curcuminoid content comparable to 50% shading. Therefore, the concentration of curcuminoids in rhizomes appears more sensitive to PAR intensity than to UV radiation exclusion (Fig. 2, inset). Furthermore, the dependence of curcuminoid concentration in rhizomes on PAR was well fitted by an exponential curve, characterized by first order constant $k = 3.0 \pm 0.1 \times 10^{-3}$ PAR^{-1}, as shown in the following equation:

$$TCC_{PAR} = TCC_{fs} + TCC_0 \times \exp^{(-k \times PAR)}$$

where TCC_{PAR} represents the total curcuminoid content (mg g^{-1}) of *Curcuma longa* as a function of PAR, TCC_{fs} represents the total curcuminoid content when plants are cultivated under full sun (0% shading), TCC_0 is the extrapolated total curcuminoid content of plants cultivated in the dark (100% shading), and k is decay kinetic constant. The decay led to a minimum curcuminoid concentration value under full sun, at about 1200 PAR (Fig. 2, inset). At this light intensity, the concentration of curcuminoids resulted about 75% with respect to plants grown under 70% shading (Fig. 2, inset). Concluding, according to our results, plants at 65 DAP under 70% shading represents the best conditions for obtaining the highest curcuminoid content in *C. longa* rhizomes (Table 1).

Noteworthy, the biomass produced at 65 DAP is about 7.5% with respect the total biomass produced at the end of growth period (see Table 1). In other words, a potential industrial plant for curcuminoid purification will treat an amount of *C. longa* rhizomes one order of magnitude lower if plants are harvested at 65 DAP, which contain 4 times higher curcuminoid content, than plants at the end of the growth period.

3.2. Binding of curcuminoids to magnetic nanoparticles

Curcuminoids present a keto-enol functionality, which shows strong binding proclivity toward a new category of maghemite nanoparticles, named Surface Active Maghemite Nanoparticles (SAMNs) (Magro et al., 2014b). Curcumin appeared as one of the best ligands for SAMN surface, among an extended list of compounds (Magro et al., 2015c), confirming the literature reporting on the formation of stable complexes between curcumin and iron(III) (Borsari et al., 2002). In the present report, based on preliminary studies (Magro et al., 2015c), an efficient curcuminoid purification process was developed exploiting the influence of solvent polarity on the binding equilibrium. Specifically, *C. longa* rhizomes, collected at 65 DAP, were manually sliced, dried at 65 °C in a ventilated oven and finely ground as described in Methods. Dried and powdered *C. longa* rhizomes were extracted (20 mg mL^{-1}) with 99.6% ethanol. Then, extracts were incubated with stable aqueous colloidal suspensions of SAMNs under magnetic stirring at room temperature for 1 h. Under optimized binding conditions, the aqueous SAMN suspension was added to the ethanol rhizome extract (3:1 v/v), thus, ethanol final concentration was 25%.

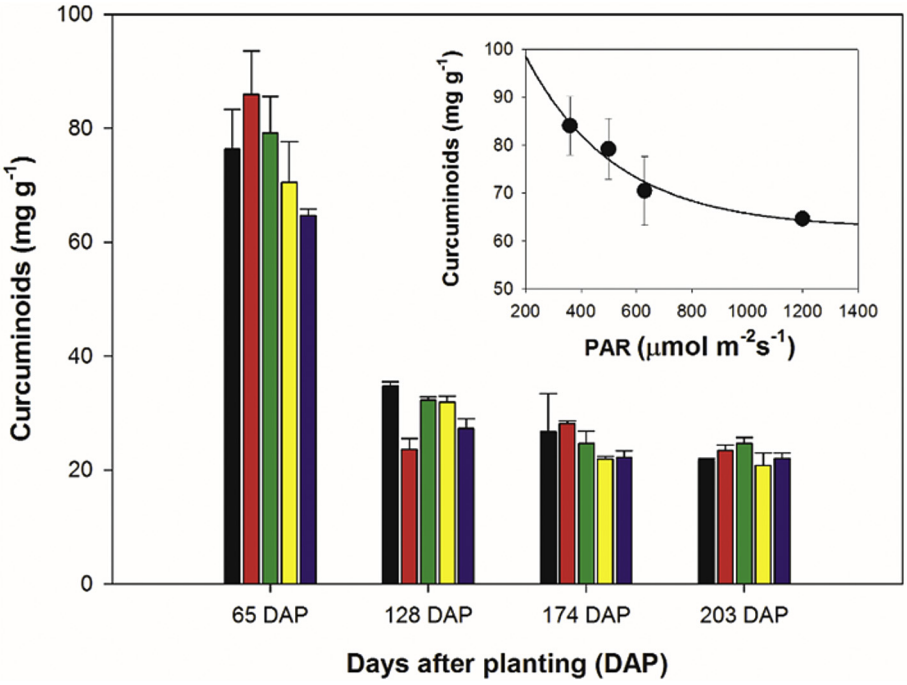

Fig. 2. Curcuminoids content (mg g^{-1}) of *C. longa* cultivated under different light conditions at different DAP. Black bars = UV radiation exclusion; red bars = 70% shading; green bars = 50% shading; yellow bars = 30% shading; blue bars = full sun. **Inset**: Curcuminoid content (mg g^{-1}) in *C. longa* rhizomes at 65 DAP as a function of PAR. The maximum error was below 3.0% for all the experimental points. (For interpretation of the references to colour in this figure legend, the reader is referred to the web version of this article.)

Table 1
Biomass (g) and curcuminoid content (% dry weight) in rhizome of *C. longa* cultivated under 70% shading at different stages of maturity (DAP).

DAP	Rhizome biomass (g)	Curcuminoids (% dry weight)
65	35.6 ± 2.3	8.4 ± 0.6
128	140.2 ± 24.6	2.5 ± 0.1
174	353.3 ± 35.7	2.8 ± 0.1
203	476.8 ± 32.0	2.3 ± 0.1

Values are the mean of six plants and three replicates with standard deviation.

Curcuminoid solubility drastically decreased with the introduction of water, and solvent modification forced the interaction of the biomolecules with nanoparticle surface. Briefly, after the incubation of *C. longa* extracts with SAMNs in 25% of ethanol, a nanobioconjugate (SAMN@curcuminoid) was produced, which was subsequently magnetically isolated and subjected to three washing cycles in water. The possible loss of bound biomolecules from the surface of SAMNs was followed by UV–Vis spectroscopy and resulted below the limit of detection of the instrument (0.25 mg L^{-1} curcuminoid). The chemical interaction between curcuminoids and SAMNs was visually witnessed by a remarkable modification of the color, from brown to red purple, of the SAMN suspension (see Fig. 3, inset).

The SAMN@curcuminoid complex was characterized by UV–Vis spectroscopy confirming the binding of the biomolecules onto the surface exposed iron(III) sites on SAMNs, as already observed in previous papers (Magro et al., 2014b, 2015b). Curcuminoid binding influenced the optical properties of SAMNs as already reported for hybrid nanomaterials, which can display peculiar properties, differently from those inherited from their components. The UV–Vis spectrum of the SAMN@curcuminoid complex was acquired and compared with those of naked SAMNs and of the *C. longa* rhizome extract (see Fig. 3). *C. longa* extract presented an intense yellow color and its spectrum was characterized by an intense band at 430 nm, attributable to the presence of curcuminoids (Rymbai et al., 2011). The electronic absorption spectrum of bare SAMNs, acquired in water, showed a wide band with a maximum at about 400 nm as already reported (Magro et al., 2012a). Conversely, the optical spectrum of the SAMN@curcuminoid complex resulted characterized by the presence of two peaks, at 350 nm and 425 nm (see Fig. 3). Such a dramatic spectral alteration, regarding both the shape and the position of the optical bands, witnessed the occurrence of the binding and provided the evidence of its covalent nature, in agreement with ESR measurement (see hereafter) and with results presented elsewhere (Magro et al., 2014b). It should be mentioned that the SAMN@curcuminoid complex was very stable in water and, if stored at 4 °C, organic molecules remained firmly bound to SAMN surface for at least 12 months.

Transmission electron microscopy (TEM) was used to further characterize the complex between magnetic nanoparticles and curcuminoids (SAMN@curcuminoid). TEM images showed the presence of an organic matrix, forming a shell of about 2.0 nm around iron oxide nanoparticles, characterized by a lower electron density, attributable to curcuminoid molecules layering on the SAMN surface (Fig. 4).

Moreover, the SAMN@curcuminoid complex was characterized by electron spin resonance (ESR) spectroscopy. In particular, ESR spectra of SAMNs and SAMN@curcuminoid were acquired in order to evidence the binding occurrence. As shown in Fig. 5, ESR spectrum of SAMNs, at room temperature, presented a nearly symmetric wide signal characterized by a center field at 2940 Gauss, corresponding to a g factor of 2.39, and a linewidth of 1200 Gauss. Differently, the ESR spectrum of the SAMN@curcuminoid complex was characterized by a center field at 2850 Gauss (g factor of 2.49) and a linewidth of 1140 Gauss. The lower linewidth indicates less magnetic interparticle interactions, and these spectral variations with respect to naked SAMNs suggest a strong binding through electron delocalization over the biomolecule–surface-iron(III)

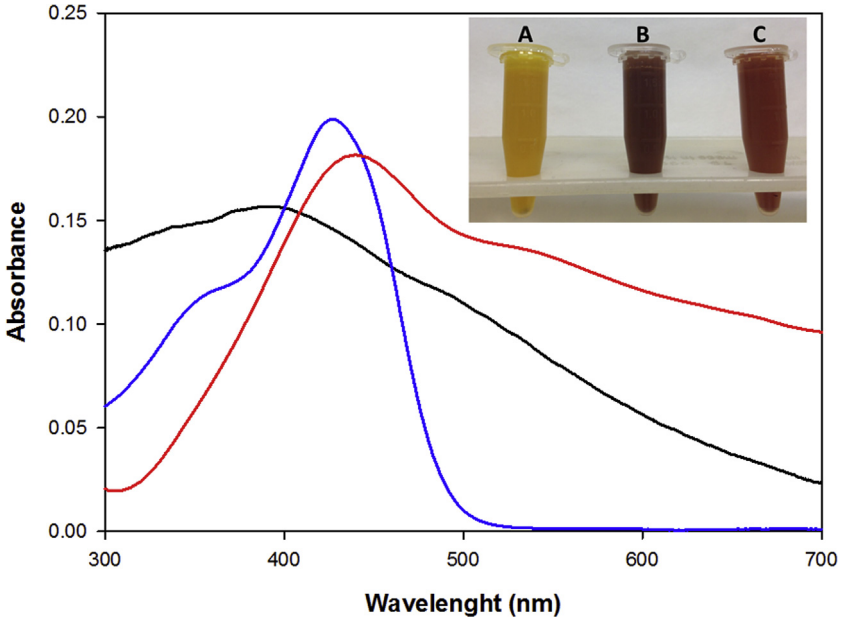

Fig. 3. UV–Vis spectra of naked and curcumin-coated SAMNs (SAMN@curcuminoid) in water. Black, 0.1 g L^{-1} SAMN; Red, 0.1 g L^{-1} SAMN@curcuminoid; Blue, 20 g L^{-1} *C. longa* extract in 25% ethanol. **Inset**. Photographs of materials used for curcumin purification. A) *C. longa* extract (20 g L^{-1}) in 25% ethanol; B) SAMN (0.1 g L^{-1}); C) SAMN@curcuminoid (0.1 g L^{-1}).

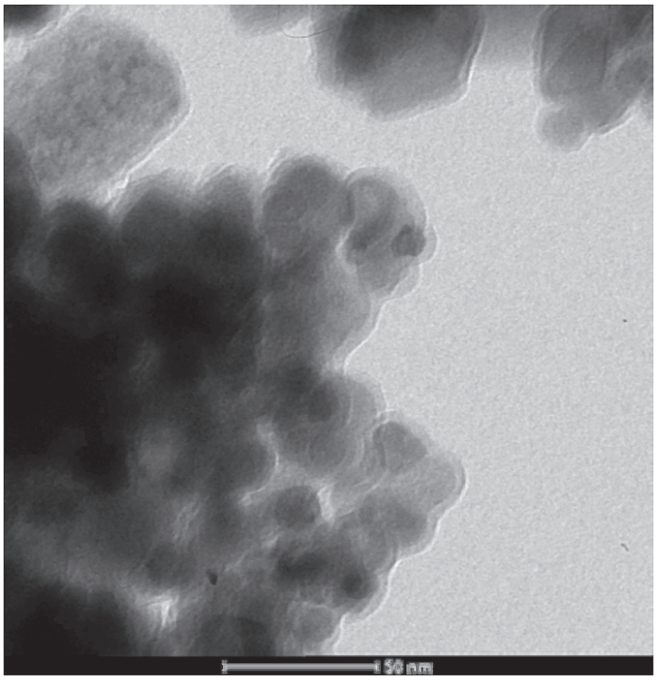

Fig. 4. Transmission electron microscopy image of SAMNs incubated in *C. longa* rhizome extracts.

complex in the SAMN@curcuminoid complex (Amstad et al., 2011).

3.3. Recovery of curcuminoids from the SAMN@curcuminoid complex

The concentration of nanoparticles during the incubation with *C. longa* rhizome extract influenced the fraction of curcuminoids released from the SAMN surface. Thus, curcuminoid binding was tested at SAMN final concentrations in the 1.0–10.0 g L^{-1} range. Interestingly, the highest yield of recovered curcuminoids was obtained with 1.0 g L^{-1} SAMNs. In particular, the fraction of bound curcuminoids, expressed in % with respect to their total amount in the extract, was 93.5% at 1.0 g L^{-1} SAMNs, while at 10.0 g L^{-1} SAMNs was 82.7% (see Table 2). This result was not surprising as at high concentrations (10 g L^{-1}) and in the presence of an organic solvent (ethanol) SAMNs can lead to partial aggregation, lowering the surface area available for binding. Thus, in the present case, the lowest SAMN concentration led to the highest colloidal stability and the highest nanoparticle surface area exposed to the solvent, and available for curcuminoid binding.

The binding process of curcuminoids to SAMN surface was very fast (completed within 5 min) and the resulting nanobioconjugate (SAMN@curcuminoid) was collected by the application of an external magnet. Then, it was extensively washed with water to eliminate loosely bound substances.

The release of curcuminoids from nanoparticle surface, after magnetic purification, was accomplished by incubating the SAMN@curcuminoid complex in 99.6% ethanol. Under these conditions, the release of curcuminoids from the nanobioconjugate was tested with different SAMN concentrations. For example, when the concentration of SAMNs in the *C. longa* rhizome extract was 1.0 g L^{-1} and 10.0 g L^{-1}, the released curcuminoids were 96.0% and 51.2% with respect to the amount of bound biomolecules, respectively (Table 2). Thus, the binding of curcuminoids on 1.0 g L^{-1} SAMNs was completely reversible, and the magnetic nanosystem was able to quantitatively bind and recover the curcuminoid molecules present in the rhizome extracts. For comparison, in a preliminary study, we described the purification of 3.95 mg curcuminoid g^{-1} *C. longa* rhizome by magnetic nanoparticles (Magro et al., 2015c). With respect to this value, in the present protocol the curcuminoid purification protocol was improved up to 69.7 mg curcuminoid g^{-1} *C. longa* rhizome, corresponding to a yield increase of about 17.5 times, using an order of magnitude lower concentration of SAMNs.

The proposed procedure for curcumin purification can be summarized as follows: dried powder of *C. longa* rhizome, collected

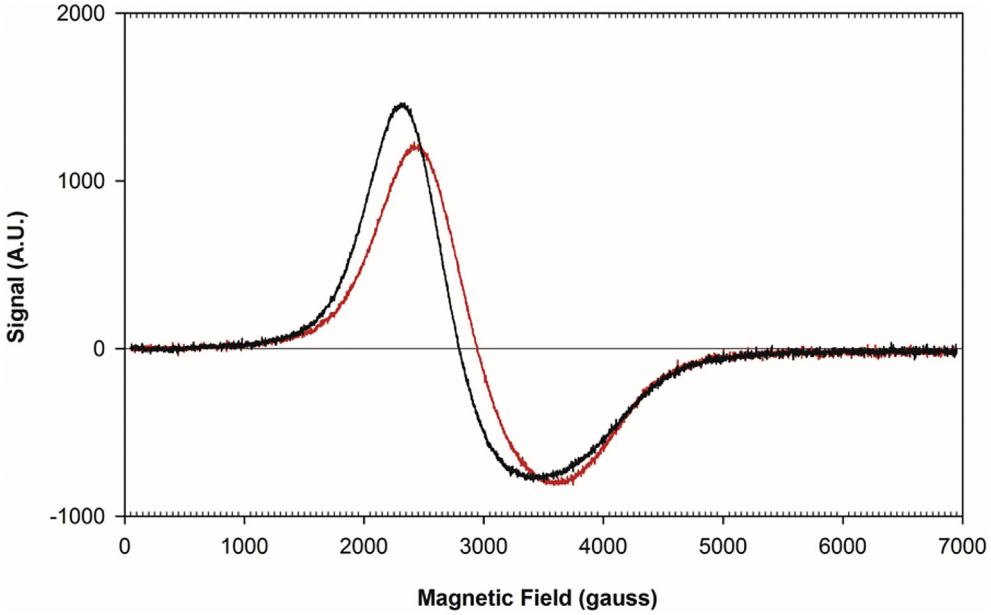

Fig. 5. Electron spin resonance spectra of SAMNs and SAMN@curcuminoid.

Table 2
Curcuminoid binding and release efficiencies in different incubations conditions with SAMNs. Bound curcuminoids were calculated with respect to their total content in the *C. longa* rhizome extracts. Purified curcuminoids were calculated with respect to their amount bound on SAMNs.

EtOH content (%)	Concentration of SAMNs (g L^{-1})	% Bound Curcuminoids	% Purified Curcuminoids
25.0	1	92.6 ± 3.7	95.5 ± 7.8
25.0	10	80.6 ± 13.8	49.9 ± 5.3
99.6	1	9.7 ± 6.1	3.2 ± 3.5
99.6	10	4.9 ± 4.2	13.8 ± 16.0

*Values are the mean and standard deviation of three experiments.

at 65 DAP, was extracted with 99.6% ethanol (1:60 w/v) aided by 5 min sonication (Falc, model LSB1, 50 kHz, 500 W). After decantation (10 min), the supernatant was incubated with SAMNs (1.0 g L^{-1}) for 5 min, under stirring, at room temperature. The nanoparticle containing suspension was subjected to magnetic separation, and the resulting supernatant was eliminated. The collected SAMN@curcuminoid complex was washed with water. The releasing of curcuminoids bound onto the nanoparticles was accomplished by subsequent incubation of SAMN@curcuminoid in 99.6% ethanol (1:60 w/v) for 1 h, at room temperature, and naked nanoparticles were magnetically removed. Under laboratory conditions, the whole process can be accomplished within 80 min. Released curcuminoids in ethanol were dried under low vacuum (100 torr) at 40 °C, leading to 67.4 ± 9.0 mg g^{-1} of a yellow powder, consisting of 47.8 ± 3.8% curcumin, 22.1 ± 2.5% demethoxy-curcumin, and 30.1 ± 3.9% bis-demethoxy-curcumin (by HPLC), with a purity > 98% with respect to the total dry rhizome mass of the extract.

After the curcuminoid purification, and due to the great reversibility of the binding, SAMNs can be recycled and used for other purification processes.

3.4. Pilot plant for curcuminoid purification by magnetic separation

Finally, with the aim of demonstrating the feasibility of the described laboratory approach to be moved to an industrial scale, a prototype plant, consisting of a simple modular and reconfigurable robotic platform, was applied for performing continuous curcuminoid purification, see Fig. 6. It should be mentioned that a modified version of this patented prototype (Magro et al., 2016d) was already described and successfully applied for environmental remediation (Magro et al., 2016e). In the current study, the system was able to process 100 L day^{-1}. Nevertheless, it is readily expandable for larger volumes in an industrial plant (Fig. 6, inset). The proposed prototype comprises two modules (a mixing module and a magnetic separation module), in which the mixing module is a paddle mixer, while the magnetic separation module is an oscillating pan, equipped with a magnetic plate for nanoparticle recovery. The magnetic plate is positioned at the bottom of the pan and the distance between the pan and the plate will vary by pneumatic actuators as the process proceeds (see Fig. 6). The module oscillations and the distance of the magnetic plate are controlled by a software built in-house. Water and SAMNs suspension were moved through the treatment steps by liquid pumps as described (Magro et al., 2016d). Note that all these operations are possible because of the peculiar colloidal stability of SAMNs, their surface reactivity, and the fast binding kinetics. In addition, the synthetic protocol for SAMNs responds to appealing requirements, such as cost effectiveness (below 3 $ g^{-1} at the laboratory scale), environmental sustainability, and industrialization suitability. The synthesis is completely carried out in water, without the necessity of any organic solvent. Moreover, SAMNs do not need any kind of cumbersome, time-consuming, and expensive stabilizing coating, which limits massive applications. Beyond their excellent characteristics in term of binding performances and low environmental impact, SAMNs represent a competitive and sustainable alternative

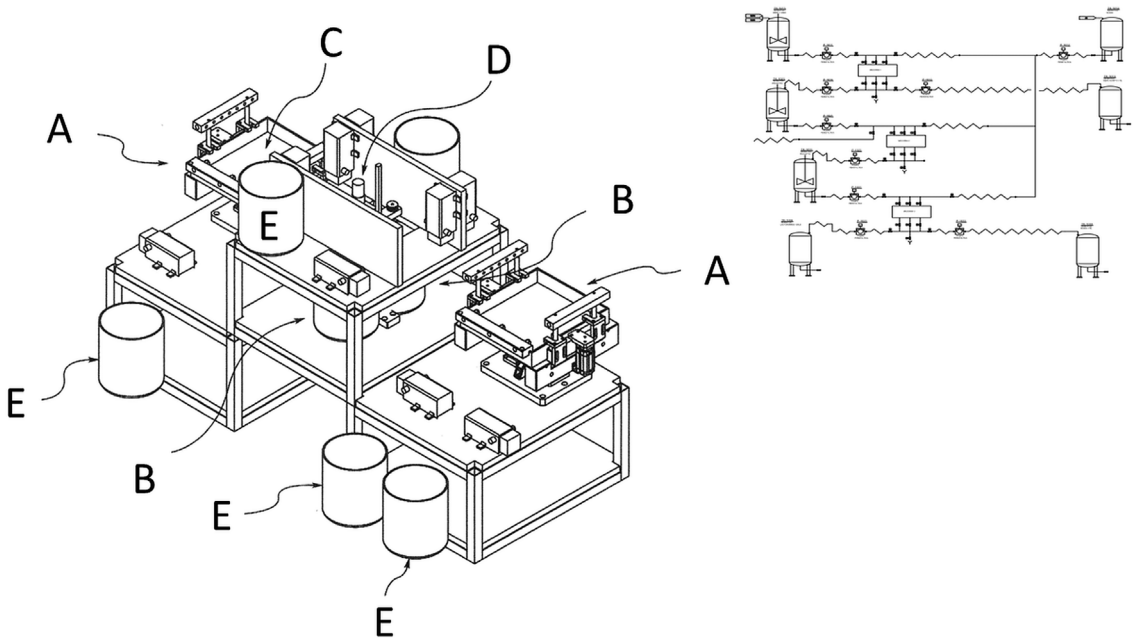

Fig. 6. Schematic representation of the pilot plant used for the recovery of curcuminoids from *C. longa* rhizome extracts by magnetic separation. A: magnetic separation module; B: mixing module; C: separation chamber; D: mixer motor; E: reservoirs for stocking water suspensions of bare SAMNs, ethanolic extract from *C. longa*, water for washing processes, recycled SAMNs, ethanol solution containing purified curcuminoids. **Inset** simplified plant scheme for the treatment of industrial scale volumes of water-ethanol extracts from *C. longa* rhizome.

to standard chromatographic or extraction methods for biomolecule purification.

4. Conclusions

The optimum harvesting time for the maximization of curcuminoid content and the reduction of biomass of *C. longa* in a case study in the Brazilian agro-climatic zone was individuated, as well as the best light exposition condition. The early harvest (65 DAP) led to 4 times higher curcuminoid content per rhizome dry weight than late harvest, reducing biological and chemical wastes as well as plant sizing to 7.5%. Moreover, a new category of maghemite nanoparticles, named Surface Active Maghemite Nanoparticles (SAMNs), was exploited for the magnetic purification of curcuminoids from *C. longa* rhizomes. The proposed magnetic purification protocol led to the recovery of 90% of high purity curcuminoids in a single magnetic purification step. Finally, an automatic modular pilot system for the continuous magnetic separation and purification of curcuminoids was applied, demonstrating the scalability of the presented approach, as SAMNs respond to essential prerequisites of environmental sustainability, and industrialization feasibility.

The reduction of biomass and the consequent waste generation, the minimization of solvent volumes and the costs related to raw material transport, as well as to the high yield and purity of curcuminoids, can be of interest for agro-industries in Brazil.

Acknowledgements

The authors gratefully acknowledge the support by Coordenação de Aperfeiçoamento de Pessoal de Nivel Superior (CAPES – Brazil), process 99999.010436/2014-06, Conselho Nacional de Pesquisa (CNPq – Brazil), process 478372/2013-2 and process 306151/2012-0 and São Paulo Research Fundation (FAPESP - Brazil), process 2013/05644-3 and 2016/22665-2. Moreover, the authors gratefully acknowledge University of Padua (Italy) grant "Assegni di Ricerca Junior" 2014 n. CPDR148959 and CARIPARO Foundation for the support. The authors thank L. Bettinsoli, M. Braga, R. Braga, and A. Gatti for the construction of the pilot plant.

References

Amstad, E., Fischer, H., Gehring, A.U., Textor, M., Reimhult, E., 2011. Magnetic decoupling of surface Fe^{3+} in magnetite nanoparticles upon nitrocatechol-anchored dispersant binding. Chem. Eur. J. 17, 7396–7398.

Asghari, G., Mostajeran, A., Shebli, M., 2009. Curcuminoid and essential oil components of turmeric at different stages of growth cultivated in Iran. Res. Pharm. Sci. 4, 55–61.

Baratella, D., Magro, M., Sinigaglia, G., Zboril, R., Salviulo, G., Vianello, F., 2013. A glucose biosensor based on surface active maghemite nanoparticles. Biosens. Bioelectron. 45, 13–18.

Bhuiyan, M.M.R., Roy, S., Sharma, P.C.D., Rashid, M.H.A., Bala, P., 2012. Impact of multistoreyed agro-forestry systems on growth and yield of turmeric and ginger at Mymensingh, Bangladesh. eSci J. Crop Prod. 1, 19–23.

Bonaiuto, E., Magro, M., Baratella, D., Jakubec, P., Sconcerle, E., Terzo, M., Miotto, G., Macone, A., Agostinelli, E., Fasolato, S., Venerando, R., Salviulo, G., Malina, O., Zboril, R., Vianello, F., 2016. Ternary hybrid γ-Fe_2O_3/Cr^{VI}/Amine Oxidase nanostructure for electrochemical sensing: application for polyamine detection in tumor tissue. Chem. Eur. J. 22, 6846–6852.

Borsari, M., Ferrari, E., Grandi, R., Saladini, M., 2002. Curcuminoids as potential new iron-chelating agents: spectroscopic, polarographic and potentiometric study on their Fe(III) complexing ability. Inorg. Chim. Acta 328, 61–68.

Camargo, N.M., Klamt, E., Kauffman, J.H., 1987. Classificação de solos usada em levantamentos pedológicos no Brasil. Bol. Soc. Bras. Ciência do Solo 12, 11–33.

Cmiel, V., Skopalik, J., Polakova, K., Solar, J., Havrdova, M., Milde, D., Justan, I., Magro, M., Starcuk, Z., Provaznik, I., 2016. Rhodamine bound maghemite as a long-term dual imaging nanoprobe of adipose tissue-derived mesenchymal stromal cells. Eur. Biophys. J. http://dx.doi.org/10.1007/s00249-016-1187-1.

Cooray, N.F., Jansz, E., Ranatunga, J., Wimalasena, S., 1988. Effect of maturity on some chemical constituents of turmeric (Curcuma longa L.). J. Nat. Sci. Found. Sri Lanka 16, 39–51.

Gupta, S.C., Kismali, G., Aggarwal, B.B., 2013. Curcumin, a component of turmeric: from farm to pharmacy. BioFactors 39, 2–13.

He, X.-G., Lin, L.-Z., Lian, L.-Z., Lindenmaier, M., 1998. Liquid chromatography–electrospray mass spectrometric analysis of curcuminoids and sesquiterpenoids in turmeric (Curcuma longa). J. Chromatogr. A 818, 127–132.

Hossain, M.A., Akamine, H., Ishimine, Y., Teruya, R., Aniya, Y., Yamawaki, K., 2009. Effects of relative light intensity on the growth, yield and curcumin content of turmeric (Curcuma longa L.) in Okinawa, Japan. Plant Prod. Sci. 12, 29–36.

Kitts, D., Weiler, K., 2003. Bioactive proteins and peptides from food sources. Applications of bioprocesses used in isolation and recovery. Curr. Pharm. Des. 9,

1309–1323.
Kulkarni, S.J., Maske, K.N., Budre, M.P., Mahajan, R.P., 2012. Extraction and purification of curcuminoids from Turmeric (Curcuma longa L.). Int. J. Pharmacol. Pharm. Technol. 1, 81–84.
Magro, M., Faralli, A., Baratella, D., Bertipaglia, I., Giannetti, S., Salviulo, G., Zboril, R., Vianello, F., 2012a. Avidin functionalized maghemite nanoparticles and their application for recombinant human biotinyl-SERCA purification. Langmuir 28, 15392–15401.
Magro, M., Sinigaglia, G., Nodari, L., Tucek, J., Polakova, K., Marusak, Z., Cardillo, S., Salviulo, G., Russo, U., Stevanato, R., Zboril, R., Vianello, F., 2012b. Charge binding of rhodamine derivative to OH^- stabilized nanomaghemite: universal nanocarrier for construction of magnetofluorescent biosensors. Acta Biomater. 8, 2068–2076.
Magro, M., Baratella, D., Pianca, N., Toninello, A., Grancara, S., Zboril, R., Vianello, F., 2013. Electrochemical determination of hydrogen peroxide production by isolated mitochondria: a novel nanocomposite carbon-maghemite nanoparticle electrode. Sens. Actuators B Chem. 176, 315–322.
Magro, M., Baratella, D., Salviulo, G., Polakova, K., Zoppellaro, G., Tucek, J., Kaslik, J., Zboril, R., Vianello, F., 2014a. Core-shell hybrid nanomaterial based on prussian blue and surface active maghemite nanoparticles as stable electrocatalyst. Biosens. Bioelectron. 52, 159–165.
Magro, M., Campos, R., Baratella, D., Lima, G., Holà, K., Divoky, C., Stollberger, R., Malina, O., Aparicio, C., Zoppellaro, G., Zboril, R., Vianello, F., 2014b. A magnetically drivable nanovehicle for curcumin with antioxidant capacity and MRI relaxation properties. Chem. Eur. J. 20, 11913–11920.
Magro, M, Valle, G., Russo, U., Nodari, L., Vianello, F., 2015a. Maghemite nanoparticles and method for preparing thereof. Patent number US Patent 8,980,218, 2015; EP 2 596 506 B1 2014.
Magro, M., Baratella, D., Jakubec, P., Zoppellaro, G., Tucek, J., Aparicio, C., Venerando, R., Sartori, G., Francescato, F., Mion, F., Gabellini, N., Zboril, R., Vianello, F., 2015b. Triggering mechanism for DNA electrical conductivity: reversible electron transfer between DNA and iron oxide nanoparticles. Adv. Funct. Mater 25, 1822–1831.
Magro, M., Campos, R., Baratella, D., Ferreira, M.I., Bonaiuto, E., Corraducci, V., Uliana, M.R., Lima, G.P.P., Santagata, S., Sambo, P., Vianello, F., 2015c. Magnetic purification of curcumin from Curcuma longa rhizome by novel naked maghemite nanoparticles. J. Agric.Agric. Food Chem. 63, 912–920.
Magro, M., Bonaiuto, E., Baratella, D., de Almeida Roger, J., Jakubec, P., Corraducci, V., Tuček, J., Malina, O., Zbořil, R., Vianello, F., 2016a. Electrocatalytic nanostructured ferric tannates: characterization and application of a polyphenol nanosensor. ChemPhysChem 17, 3196–3203.
Magro, M., Moritz, D.E., Bonaiuto, E., Baratella, D., Terzo, M., Jakubec, P., Malina, O., Cepe, K., De Aragao, G.M.F., Zboril, R., Vianello, F., 2016b. Citrinin mycotoxin recognition and removal by naked magnetic nanoparticles. Food Chem. 203, 505–512.
Magro, M., Fasolato, L., Bonaiuto, E., Andreani, N.A., Baratella, D., Corraducci, V., Miotto, G., Cardazzo, B., Vianello, F., 2016c. Enlightening mineral iron sensing in Pseudomonas fluorescens by surface active maghemite nanoparticles: involvement of the OprF porin. Biochim. Biophys. Acta 1860, 2202–2210.
Magro, M., Bettinsoli, L., Braga, M., Braga, R., Gatti, A., Vianello, F., 2016d. Apparatus and method for a separation through magnetic nanoparticles. Patent number WO 016/157027 A1.
Magro, M., Domeneghetti, S., Baratella, D., Jakubec, P., Salviulo, G., Bonaiuto, E., Venier, P., Malina, O., Tuček, J., Ranc, V., Zoppellaro, G., Zbořil, R., Vianello, F., 2016e. Colloidal Surface Active Maghemite Nanoparticles for biologically safe Cr^{VI} remediation: from core-shell nanostructures to pilot plant development. Chem. Eur. J. 22, 14219–14226.
Manhas, S.S., Gill, B.S., 2012. Effect of different cultural practices on production of turmeric (Curcuma longa L.) in Punjab. J. Spic. Arom. Crops 21, 53–58.
Miotto, G., Magro, M., Terzo, M., Zaccarin, M., Da Dalt, L., Bonaiuto, E., Baratella, D., Gabai, G., Vianello, F., 2016. Protein corona as a proteome fingerprint: the example of hidden biomarkers for cow mastitis. Colloids Surf. B 140, 40–49.
Nair, K.P.P., 2013. The botany of turmeric. In: Nair, K.P.P. (Ed.), The Agronomy and Economy of Turmeric and Ginger: the Invaluable Medicinal Spice Crops. Elsevier Scientific Publishing Company, Amsterdam, pp. 7–32.
Padmapriya, S., Chezhiyan, N., Sathiyamurthy, V.A., 2007. Effect of shade and integrated nutrient management on biochemical constituents of turmeric (Curcuma longa L.). J. Hortic. Sci. 2, 123–129.
Rymbai, H., Sharma, R.R., Srivastav, M., 2011. Biocolorants and its implications in health and food industry-a review. Int. J. PharmTech Res. 3, 2228–2244.
Santos, H.G., Jacomine, P.K.T., Anjos, L.H.C., Oliveira, V.A., Oliveira, J.B., Coelho, M.R., Lumbreras, J.F., 2006. Sistema brasileiro de classificação de solos, second ed. Embrapa solos, Rio de Janeiro.
Sinigaglia, G., Magro, M., Miotto, G., Cardillo, S., Agostinelli, E., Zboril, R., Bidollari, E., Vianello, F., 2012. Catalytically active bovine serum amine oxidase bound to fluorescent and magnetically drivable nanoparticles. Int. J. Nanomed 7, 2249–2259.
Skopalik, J., Polakova, K., Havrdova, M., Justan, I., Magro, M., Milde, D., Knopfova, L., Smarda, J., Polakova, H., Gabrielova, E., Vianello, F., Michalek, J., Zboril, R., 2014. Mesenchymal stromal cell labeling by new uncoated superparamagnetic maghemite nanoparticles in comparison with commercial Resovist – an initial in vitro study. Int. J. Nanomed 9, 5355–5372.
Srikrishnah, S., Sutharsan, S., 2015. Effect of different shade levels on growth and tuber yield of turmeric (Curcuma longa L.) in the Batticaloa District of Sri Lanka. Am. Euras. J. Agric.Agric. Environ. Sci. 15, 813–816.
Turková, J., 1978. Affinity Chromatography, first ed. Elsevier Scientific Publishing Company, Amsterdam.
Urbanova, V., Magro, M., Gedanken, A., Baratella, D., Vianello, F., Zboril, R., 2014. Nanocrystalline iron oxides, composites, and related materials as a platform for electrochemical, magnetic, and chemical biosensors. Chem. Mater 26, 6653–6673.
Venerando, R., Miotto, G., Magro, M., Dallan, M., Baratella, D., Bonaiuto, E., Zboril, R., Vianello, F., 2013. Magnetic nanoparticles with covalently bound self-assembled protein corona for advanced biomedical applications. J. Phys. Chem. C 117, 20320–20331.